Polymer 51 (2010) 1585–1592

Contents lists available at ScienceDirect

Polymer

journal homepage: www.elsevier.com/locate/polymer

Investigation of nanostructures and properties of sulfonated poly(arylenethioethersulfone) copolymer as proton conducting materials by small angle neutron scattering

Mitra Yoonessi [a,1], Thuy D. Dang [a], Hendrik Heinz [b], Robert Wheeler [b], Zongwu Bai [c,*]

[a] Air Force Research Laboratory, AFRL/RXBN, Wright-Patterson AFB, OH 45433, USA
[b] Department of Polymer Engineering, University of Akron, Akron, OH 44325, USA
[c] University of Dayton Research Institute, University of Dayton, Dayton, OH 45469, USA

ARTICLE INFO

Article history:
Received 28 October 2009
Received in revised form
2 February 2010
Accepted 7 February 2010
Available online 12 February 2010

Keywords:
Sulfonated polymers
Water absorption
Proton transport

ABSTRACT

Sulfonated poly(arylenethioethersulfone) copolymer (SPTES-50), a promising candidate material for proton exchange membrane fuel cell (PEMFC), exhibited excellent thermal stability, high proton conductivity (135 mS/cm at 85 °C, 85% relative humidity), and electrochemical property. Small angle neutron scattering (SANS) of fully hydrated SPTES-50 membranes revealed the presence of embedded spherical nanodomains containing ionic group and water within the polymer membranes. The polydispersity of the nanoscale structure limited scattering contrast between the polymer backbone and sulfonated groups, and precluded analysis of intermediate and large scattering vectors in terms of the polymer–water interface structure. Inter-cluster correlations associated with the large extent of water absorption in the fully hydrated SPTES-50 membranes were accounted by Percus–Yevick liquid-like ordering of polydispersed hard sphere model with Schulz polydispersity approximation. Approximation of their low q upturn with an exponential decay results in a decay of −3 at 25 °C accounted for inter-cluster correlations which changed to a decay of −1.1 at 55 °C and 77 °C. This indicated a change in morphology upon increase of temperature such as to fractal morphology or an interconnected cylindrical network. The scattering patterns don't exhibit any further changes within examined range of q when the temperature increased from 55 °C to 77 °C. The number density of ionic clusters remained approximately constant ($\sim 1.1818 \times 10^{17}$ cm^3), which indicated that additional water adsorbed by the polymer at the elevated temperature did not result in substantial coalescence of the clusters. Transmission electron microscopy (TEM) observation of the silver exchanged SPTES-50 membranes exhibited aggregates of Ag^+ embedded within the dry membranes which can be approximated by isolated spheres.

1. Introduction

The increasing demand for the new source of energy for internal combustion engine of vehicles, telecommunication and portable devices, laptops, and cell phones requires developing new green methods of energy generation such as fuel cells. Proton exchange membrane (PEM) is a critical component of hydrogen fuel cell which separate gases from mixing while maintaining a path for proton transport. Key properties of PEM materials are high proton conductivity, good electrochemical properties, durability, excellent thermal stability, low permeation to reactant gases (hydrogen and oxygen) and small dimensional variations upon hydration–dehydration cycles. Nafion membranes are limited by high cost, high permeation of methanol, loss of proton conductivity at high temperatures (>80 °C) and low relative humidity (<50%). The last two effects result from membrane dehydration and low glass transition temperature of Nafion (T_g: 110–130 °C) [1,2]. A range of sulfonated polymers with aromatic phenyl ring in the backbone such as sulfonated polyetherether ketone (SPEEK) [3], sulfonated polyimide (SPI) [4,5], sulfonated polysulfones [6,7] and sulfonated polybenzimidazole [8] have been developed and investigated to overcome Nafion's limitations. Proton conductivity of these membranes depends on the degree of sulfonation, number of water molecules associated with one sulfonic group and their activity. These polymers in general possess higher thermal stability and lower methanol crossover (for direct methanol fuel cells).

* Corresponding author. Tel.: +1 937 255 9116; fax: +1 937 258 8075.
E-mail address: zongwu.bai@wpafb.af.mil (Z. Bai).
[1] Present address: Ohio Aerospace Institute, 22800 Cedar Point Rd., Cleveland, OH 44142, USA.

0032-3861/$ – see front matter © 2010 Elsevier Ltd. All rights reserved.
doi:10.1016/j.polymer.2010.02.011

Sulfonated poly(arylenethioethersulfone) copolymer (SPTES-50) membranes have good processability, and excellent thermal and electrochemical properties as well as low cost to make [9–11]. SPTES-50 is a sulfonated poly(arylenethioethersulfone) copolymer with equal ratio of hydrophobic and hydrophilic chain segment ratio (see Fig. 1). It posses key characteristics of high proton conductivity (135 mS/cm at 85 °C, 85% relative humidity (RH)), low gas permeation rate, and thermal stability (T_g ~ 200 °C). The presence of sulfonated groups on the backbone containing aromatic phenyl rings leads to lower segregation of hydrophobic and hydrophilic compared to Nafion where the sulfonated groups are in the pendant chain of a flexible polymer backbone. The polycondensation synthesis of SPTES copolymers with tailored hydrophobic and hydrophilic chain segment ratio has been described elsewhere [10,11]. SPTES-50 membrane can be incorporated into a membrane electrode assembly for hydrogen fuel cell operations and it can operate at elevated temperatures (>100 °C) when water molecules are present.

Sulfonated polymers phase separate to form hydrophobic domains and aggregates of sulfonic groups which contain water molecules and hydronium ions [12]. The macromolecular architecture and the degree of sulfonation control the size and structure of the phases. The dynamics and transport of proton and hydronium ions depend on the strength of the ionic interactions between hydronium ions and sulfonic groups, water activity, inter-aggregate distance and connectivity of the aggregates. Characteristics of Nafion have been examined extensively including proton conductivity and its dependence on temperature and humidity, diffusion coefficient by pulsed-gradient NMR and structural models by SANS and combination of experimental structural analysis and simulations of reconstruction by SAXS [13–16].

Numerous models such as sphere [17], core–shell [18], parallelpiped [19], and local order model [5,20,21] have been introduced to explain cluster size and water aggregate network formation at high water contents semi-quantitatively. More recently, it was shown that Nafion forms randomly packed inverted micelle cylindrical structure [22,23]. The effects of external counter ion on the internal structure of the ionomeric aggregates and clusters of Nafion have been studied extensively. Few studies on a range of swollen states from dry to solution have suggested an inverted micelle model for low water content and a network of rod-like polymer aggregates for dilute solution [13]. There is no semi-quantitative information available regarding the structure of sulfonated poly(arylenethioethersulfone)s to the best of our knowledge. Preliminary X-ray scattering (SAXS) and AFM studies of the SPTES copolymer (SPTES-70) membranes indicated a phase separation between hydrophobic and hydrophilic segments [9], and significant differences between the nanostructures of SPTES membranes in comparison to Nafion. SAXS studies of the SPTES-70 revealed the presence of a broad maximum corresponding to the sulfonic aggregates where the size depends on the membrane hydration. Presence of a broader peak suggests a lower degree of segregation between hydrophobic and hydrophilic domains. This could be attributed to the lower flexibility of the polymer chain and the presence of sulfonic groups on the polymer backbone. This study attempts to investigate and quantify the nanostructure of hydrated SPTES-50 membrane and to provide a correlation between its phase morphology and its proton conductivity.

2. Experimental

2.1. Materials

A solution (~10 wt%) of SPTES-50 (equivalent weight of 610 g/eq.) in dimethyl acetamide (DMAc, Sigma Aldrich) was filtered several times, cast in a flat dish and placed in vacuum oven with a gradual temperature increase to 100 °C for 24 h and 120 °C for 2 h. The resulting uniform flat membranes immersed in deionized water for 2 h and dried under vacuum (24 h, 80 °C) after they were acidified in sulfuric acid (4 M, 24 h) to ensure complete conversion of sulfonic groups to their protonated forms.

2.2. Characterization

Membranes were dried in vacuum (80 °C and 20 mb) (W_{dry}), and then immersed in DI water at 25 °C, 55 °C, and 77 °C (accuracy of 0.5 °C) for 2 h until constant weight was achieved (W_h). The reported water uptake of the membrane was determined from the weight of the hydrated membrane and weight of the dry membrane as follow equation (1):

$$\text{Water uptake} = \frac{W_h - W_{dry}}{W_{dry}} \times 100\% \quad (1)$$

The volume fraction of water (ϕ_w) was obtained from the equation (2):

$$\phi_w = \rho_p W_w / \left(\rho_{H_2O} W_{dry} + \rho_p W_w\right) \quad (2)$$

where W_w is the weight of water, ρ_p and ρ_{H_2O} are the density of dry polymer and water, respectively. Reported water volume fractions are average of three independent measurements. Compared to a previous study [9], we have obtained a higher water volume fraction which may be associated with a different rate of solvent evaporation during film formation or differences in polymer batches such as monomer sequence in the copolymer backbone, degree of polymerization, and polydispersity.

Measurements of the proton conductivity were performed using AC impedance spectroscopy with an Alpha High Resolution Dielectric/Impedance Analyzer (Novo Control), over frequency range of (10 Hz–1 MHz) using a standard 4-electrode setup. The impedance values in a range of zero phase angles were used to calculate the proton conductivity (σ), as follow equation (3):

$$\rho = l/RS \quad (3)$$

where l is the distance between electrodes in cm, R is the resistance, S is the cross sectional area in cm^2 and σ is proton conductivity in S/cm.

The SANS experiments were performed at the National Institute of Standards and Technology (NIST), Neutron Center for Research on the 30 m NG-7 SANS instrument with a neutron wavelength, λ, of 6 Å ($\Delta\lambda/\lambda = 10\%$) and three sample-to-detector distance of 1.5 m, 10 m ($\lambda = 6$ Å), and 15 m ($\lambda = 8$ Å), $0.001 < q < 0.3168$ $Å^{-1}$ at 25 °C, 55 °C, and 77 °C (accuracy of 0.5 °C). Hydrated membranes were placed in demountable 1 mm thick titanium liquid cells filled with D_2O after equilibrium in D_2O (24 h). Scattered intensities were reduced, corrected for the transmission and background and placed on absolute scale. Then, circularly averaged to produce absolute scale scattering intensity, $I(q)$, as a function of the wave vector, q,

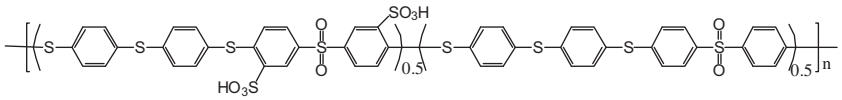

Fig. 1. Chemical structure of sulfonated endcapped poly(arylenethioethersulfone) copolymer (SPTES-50).

where $q = (4\pi/\lambda)\sin(\theta/2)$ and θ is the scattering angle. Calculations were performed using Igor Pro® software.

High Resolution TEM (HR-TEM) analyses were conducted using a Philips CM200 Field Emission Gun (FEG) instrument operating at 200 kV. The acid form of SPTES-50 membrane was treated with NaOH (1 M) for 1 h, and then exchanged with Ag by placing the SPTES-50 membrane in silver nitrate solution (0.5 M) for 24 h. Dried Ag exchanged SPTES-50 membrane was embedded in epoxy and ultramicrotomed (thickness ~25 nm). Particle size measurements were performed using Scion Image® software (accuracy of ±0.5 nm).

3. Theory

SANS background are presented for the clarity of data analysis. The scattering event with neutrons is the result of elastic interactions of the neutrons with atomic nuclei in contrast to the interaction of light or X-ray with locally variable light and electron density. The scattering cross section is a measure of the strength of the interactions between neutrons and atomic nuclei. The neutron–nucleus interaction differs significantly for isotopes of the same atom, especially when the atomic number density is low as for hydrogen and deuterium. This can be used to distinguish scattering from certain features of the structure by deuterium labeling or using a deuterated solvent. The scattering length density ρ_j is defined as equation (4):

$$\rho_j = \sum b_j N/V_m \tag{4}$$

where b_j is the scattering length of atom j, N is the Avogadro number and V_m is the molar volume.

The intensity of scattering for monodisperse particles is defined as equation (5) [24,25]:

$$I(\vec{q}) = \frac{d\sum(\vec{q})}{d\Omega} = K\cdot P(\vec{q})\cdot S(\vec{q}) \tag{5}$$

Hereby, K is an instrumental constant, $P(q)$ is the form factor arising from the shape of particle, and $S(q)$ is the structural factor of the particle related to particle–particle interactions.

The form factor for a sphere has been described as $P(q) = \phi_w V_p (\Delta\rho)^2 [\Phi(q, R)]^2$, where ϕ_w is the water volume fraction, V_p is the volume of particles, $\Delta\rho$ is the contrast, R is the sphere radius, q is the wave vector and Φ is defined according to equation (6).

$$\Phi(q,R) = \frac{3(\sin(qR) - qR\cos(qR))}{(qR)^3} \tag{6}$$

The form factor described above is accurate for systems of monodispersed spheres. In describing most of the practical systems, the polydispersity in shape and size are important factors contributing to the scattering event. Size polydispersity eliminates the high q oscillation and results in smearing scattering at high q. Therefore, size polydispersity has been frequently included in the scattering in terms of Gaussian or Schulz distribution function to take into account the Porod oscillations [25]. The probability density function of Schulz distribution function has been incorporated to describe the polydispersity of the form factors used in this study as follows equations (7) and (8).

$$\overline{I(q)} = \int_0^\infty I(q,r)P(r,R_c,z)dr \tag{7}$$

$$P(r) = \left[\frac{(z+1)^{z+1}}{R_c}\right]\frac{r^z}{\Gamma(z+1)}\exp\left[-\frac{(z+1)R}{R_c}\right] \tag{8}$$

where $\Gamma(z)$ is the gamma function, R_c is the average particle radius, z is the width parameter related to σ, the root mean square deviation of the radius ($\sigma = R_c/\sqrt{(z+1)}$, i.e. σ/R_c is the polydispersity index.

3.1. Hard spheres with liquid-like ordering (Percus–Yevick approximation)

When the density of scatterers increase such that the distance between scatterers is comparable to the size of the scatterer, pair correlations must be taken into consideration ($S(q) \neq 1$). The structural factor is an average overall orientation for isotropic scatterers [6,25]. The spatial organization of the particles depends on the interparticle potential which can be calculated from statistical mechanics. The interference factor (structural factor) is given by equation (9) where $n = \phi_s/V_s$ is the particle number density and $g(r)$ is the radial distribution function describing the arrangement of spherical particles [26].

$$\langle S(\vec{q})\rangle = S(q) = 1 + 4\pi n\int_0^\infty (g(r)-1)\frac{\sin(qr)}{qr}r^2dr \tag{9}$$

Correlation function, $g(r)$, can be calculated from interparticle potential using statistical mechanics and liquid-state theory; therefore structural factor can be calculated. Total correlation function of $h(r)$ is the sum of direct correlation, $c(r)$ and all other correlations according to Ornstein and Zernike equation (10).

$$h(r) = g(r) - 1 = c(r) + n\int c(r)h(r)dr \tag{10}$$

Two general approaches can be found to derive $S(q)$. For spherical symmetry and an intermediate degree of order characterized by liquid-like correlations of the position of the spheres, $S(q)$ has the general form of $S(q) = 1/(1 - nC(q))$. Kinning and Thomas obtained an analytical derivation of liquid-like order using Percus–Yevick closure [27].

3.2. Quantifying interface

The scattering in a two-phase system at the interface can be described by the Porod law [24] as follows equation (11):

$$\lim_{q\to\infty} I\cdot q^4 = 2\pi\Delta\rho^2\sum = \frac{\sum(\mathrm{INV})}{\pi\phi_w(1-\phi_w)} \tag{11}$$

where I is the scattering intensity, q is the wave vector, $\Delta\rho$ is the contrast, $\sum$ is the interfacial area per unit of scattering volume (surface to volume ratio), and INV is the scattering invariant. The interfacial area per unit volume obtained from this analysis obtained from a direct analysis and it is model independent. Direct geometrical information can be obtained assuming particle shape and geometry is known. This Porod limiting value is directly related to the scattering invariant (INV) and the volume fraction of the second phase (ϕ_w). Scattering invariant for a two-phase system is defined as equation (12) [25]:

$$\mathrm{INV} = \int_0^\infty q^2 I(q)dq = 2\pi^2(\Delta\rho)^2\phi_w(1-\phi_w) \tag{12}$$

4. Results and discussion

4.1. Structures and properties of SPTES-50

SPTES-50 has a proton conductivity of 135 mS/cm at 85 °C and 85% RH, an ion exchange capacity of 1.64 meq./g (610 g/eq.) *versus* 0.91 meq./g (1100 g/eq.) of Nafion, a high degree of sulfonation

Table 1
Conductivity and water uptake data for SPTES-50 copolymer and Nafion-117.

Sample	EW (g/equiv)	IEC meq./g	Sulfonation degree (%)	Conductivity mS/cm @ 85 °C, 85% RH	Water uptake, wt% (25 °C)	E_a activation energy[a]
SPTES-50	610	1.64	45.05	135	47	4.2
Nafion-117	1100	0.91	N/A	101	19	2.2

[a] Activation energy calculated based on Arrhenius relationship at 85% RH.

(45.05%), and a water uptake of 47 wt% *versus* 19 wt% as of Nafion-117 at 25 °C (see Table 1). The Arrhenius estimation [28,29] ($\sigma = Ae^{-E_a/RT}$; σ: proton conductivity; A: constant; E_a activation energy) of proton transport activation energy for SPTES-50 and Nafion-117's results in 4.22 kcal/mol and 2.12 kcal/mol, respectively (see Fig. 2). A study of SPTES-50 proton conductivity as a function of relative humidity and temperature suggests a proton conductivity that strongly depends on the temperature and relative humidity (see Fig. 3). At low relative humidities (35–65% RH), the proton conductivity of SPTES-50 is not significant (0.25–20 mS/cm). However, increasing the relative humidity to 75% resulted in increased proton conductivity to 30 mS/cm at 55 °C and continued to rise with increasing temperature (63 mS/cm at 85 °C). At high relative humidity, 85%, the proton conductivity of SPTES-50 was significantly increased to 135 mS/cm when temperature increased to 85 °C. This study suggests a proton conducting mechanism that strongly depends on the presence of water molecules at elevated temperatures. This can be attributed to the higher thermal diffusion of hydronium ions and water molecules through the expanded nanodomains and channels.

Increased proton conductivity at high temperatures and high relative humidities suggests the presence of a proton conducting mechanism which is highly dependent on the temperature and polymer's hydration state. Therefore, it is crucial to provide an understanding of the polyelectrolyte nanostructure and morphology at different temperatures. This gave motivation to further examine the membrane's nanostructure using high resolution transmission electron microscopy (HR-TEM) and small angle neutron scattering.

4.2. Morphology and properties of SPTES-50 membranes

HR-TEM examination of SPTES-50–Ag illustrated a dispersion of dark spherical nanoparticles embedded within the SPTES-50 membrane (see Fig. 4). Identification of the elements with X-ray scans, photon energies, illustrated the presence of C (Kα = 0.277 KeV), O (Kα = 0.532 KeV), S (Kα = 2.310 KeV), Ag (Lα_1 = 2.984 KeV), and Cu (Lα_1 = 8.048 KeV) in the examined area (see Fig. 4). The photon energy obtained from spherical nanoparticles was Lα_1 = 2.984 KeV corresponding to Ag. The presence of C, O, and S was expected from the constituents of the polymer backbone. The presence of silver was attributed to proton exchange at the sulfonic sites in the ionic domains for Ag^+ ions. According to the shape (see Fig. 4), Ag^+ or H^+ cations in ionic aggregates were localized in near-spherical nanodomains embedded in the polymer matrix. The domain size range of the cation (H^+ or Ag^+) exchanged SPTES-50 membrane is in the order of few nanometers depending on the valence and size of the exchanged ion and the extent of the presence of water molecules (membrane hydration). The contrast between the particles is attributed to their position in z direction whereby nanoparticles closer to the surface exhibit higher contrast and appear darker and particles deeper below the surface exhibit lower contrast. Analysis of particle size distribution in the bright field electron micrographs resulted in a mean radius of 3.3 nm and σ standard deviation of 0.81 (σ_{eff} = 24.5%).

The preparation of samples was performed by immersion of the membranes in electrolyte at 25 °C followed by drying, embedding in epoxy resin and ultramicrotoming. The membranes can be prepared at 55 °C and 77 °C by increasing the electrolyte solution temperature to 55 and 77 °C, followed by placing in liquid nitrogen, freeze drying, embedding in epoxy resin, and then microtoming. This could allow examination of the structure at 55 and 77 °C.

4.3. Small angle neutron scattering study of SPTES-50 membrane

Table 2 summarizes the material properties and characteristics of the samples placed in the beam. The scattering length density of the SPTES-50 membrane is 1.75 × 10^{-6} Å^{-2} and as of D_2O is 6.33 × 10^{-6} Å^{-2} which result in a contrast $\Delta\rho$ of 4.58 × 10^{-6} Å^{-2}

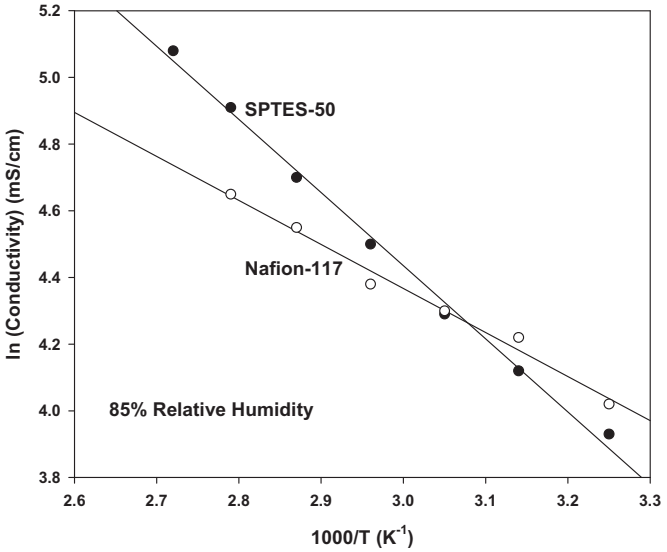

Fig. 2. The proton conductivity of SPTES-50 from 35 °C to 95 °C at 85% relative humidity.

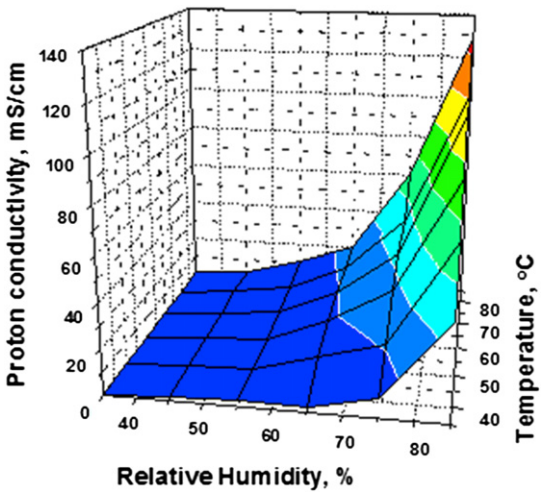

Fig. 3. Proton conductivity of SPTS-50 as a function of temperature (35–85 °C) and relative humidity (35–85%).

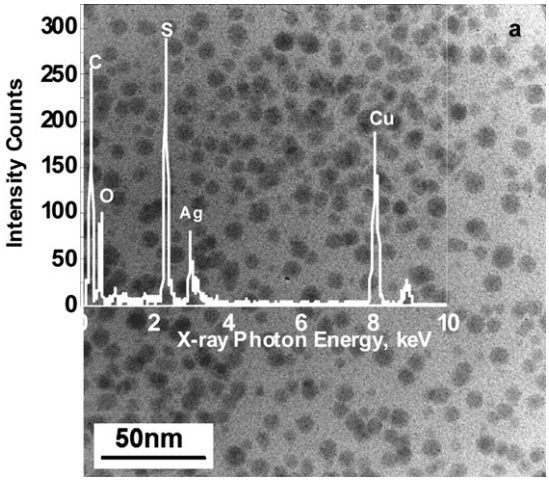

Fig. 4. Bright field high resolution TEM micrograph and X-ray spectra of the silver exchanged SPTES-50 membrane obtained from Ag–SPTES-50 (R_c = 33 Å, σ_{eff} = 24.5%).

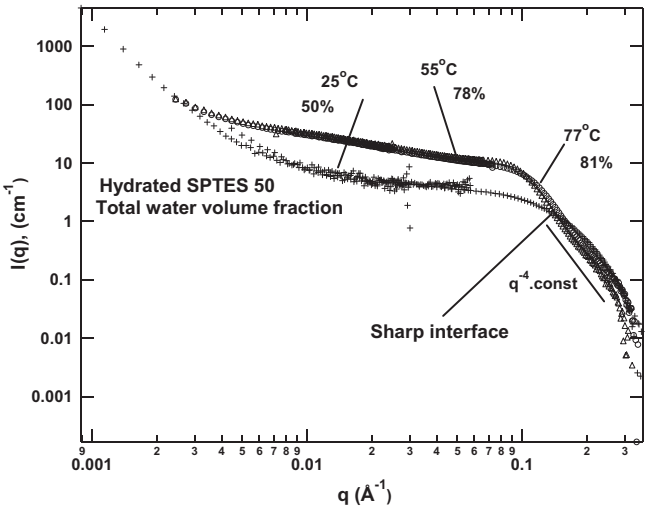

Fig. 5. SANS patterns of fully hydrated (D_2O) SPTES-50 membrane at 25 °C (+), 55 °C (○), and 77 °C (△).

(see Table 2). Fig. 5 shows the background subtracted SANS data from the D_2O hydrated SPTES-50 membrane at 25 °C, 55 °C and 77 °C. The small angle scattering region contains the low frequency scattering length density fluctuations composed of contribution from larger scale microphase morphology. The scattering intensity increased with the inclusion of water in the films and more significantly with increasing temperature. The high q regime contains higher frequency fluctuations from the contribution of nanophase structures up to wide angle regime from contribution of contrast between nuclei–nuclei. The presence of medium range q scattering is due to the existence of a second phase within the polymer matrix which has a contrast with the polymer matrix and gives rise to the scattering observed in the high q range. This system contains water molecules entrapped in the sulfonic domains and polymeric phase, which can be analyzed as a two-phase system.

The scattering profile of hydrated SPTES-50 membrane at 25 °C membranes does not exhibit well-defined scattering maxima as reported for perfluorosulfonated ionomer. The onset of peak formation is observed when the temperature is increased to 55 °C and 77 °C. This indicates that no defined packing order of the ionic aggregates exists at 25 °C. Absence of well-defined maxima is most likely due to the two main factors. First, lower flexibility of the SPTES copolymer backbone which makes the segregation of the hydrophobic and hydrophilic domains more difficult. Second, the presence of sulfonated groups on the main polymer backbone compared to the perfluorosulonated ionomers (PFSI) where the sulfonated groups are located in the pendants. The lower flexibility of the backbone combined with the presence of sulfonated groups on the main chain result in less segregated and less ordered structure of the ionic domains containing water molecules. The large angle scattering spectra of hydrated SPTES-50 membrane at 25 °C exhibited a scattering feature which could be described as polydisperse spherical nanodomains with presence of particle–particle interactions. The low angle scattering spectra of this membrane has an upturn in the low q region resulting from the correlation lengths existing between water inclusion ionic domains. The low q upturn indicates the existence of a correlation between scatterers. The scattering spectra of the membrane show an asymptotic behavior of q^{-4} in log–log scale at large angles indicating the presence of a well-defined water–polymer interface [4,13]. The formation and presence of ionic aggregates and their sizes are mostly dictated by the polymer–water interfacial phenomena. The polymer–solvent interfacial energy changes the ionic aggregate size and their spatial distribution.

As the temperature increased from 25 °C to 55 °C and 77 °C, the scattering intensity increased due to the increased volume of scatterers (water molecules) in the membrane (see Fig. 5). The increase in the scattering intensity of hydrated SPTES-50 membrane at 55 °C compared to 25 °C is attributed to the volume expansion of the ionic domains containing water molecules resulted from an increase in the diffusion coefficient and diffusion rate of water molecules into the ionic aggregates. The large angle scattering spectra of hydrated SPTES-50 membrane at the 55 °C exhibited a more defined scattering spectra indicating the existence of correlation length between the ionic clusters and an increase in excluded volume by increased volume of the hard spheres.

4.3.1. Hydrated SPTES-50 membrane at 25 °C

The polydisperse hard sphere model with Percus–Yevick liquid-like ordering with a low q power law decay describes the experimental SANS data from hydrated SPTES-50 membrane at 25 °C in the $0.0009 < q < 0.3$ 1/Å (see Fig. 6). It is assumed that the water molecules are segregated in nanophase domains embedded in the polymer matrix in spherical domains. The difference in the scattering length density of SPTES-50 ($C_{24}H_{16}O_5S_5$, 1.75×10^{-6} Å^{-2}) and

Table 2
SPTES-50 membrane and material properties and characteristics.

	SPTES-50 (dry)	Hydrated SPTES-50 at 25 °C	Hydrated SPTES-50 at 55 °C	D_2O	H_2O
Atomic composition	$C_{24}H_{16}O_5S_5$	$C_{24}H_{16}O_5S_5$	$C_{24}H_{16}O_5S_5$	D_2O	H_2O
Scattering length density[a] (10^6 Å^{-2})	1.75	1.75	1.75	6.33	−5.6
Contrast ($\Delta\rho$, 10^6 Å^{-2})		4.58	4.34		
Water volume fraction (ϕ_w, %)[b]	6–7	50	78		

[a] See equation (4).
[b] Water content of the dry sample was measured after equilibrium with air containing 22% RH, while as of hydrated sample was measured after 24 h relative to the vacuum oven (20 mb, 80 °C) dried weight equilibrium (average of 4 samples).

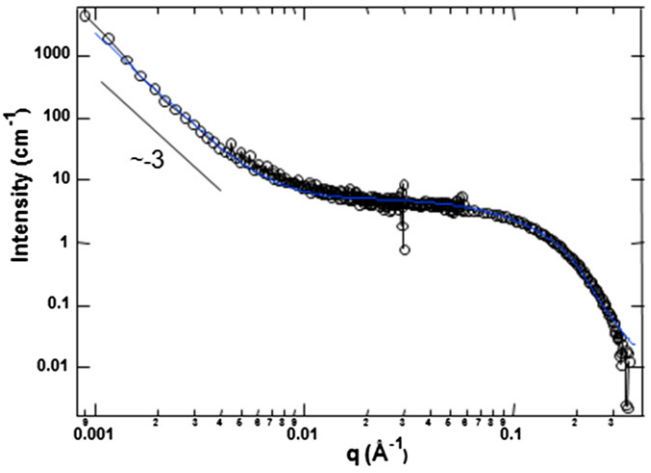

Fig. 6. Comparison of the SANS patterns of hydrated SPTES-50 at 25 °C (○) with an optimized model of hard polydisperse spheres with liquid-like (Percus–Yevick) ordering assuming $R_{HS} = R$ (solid blue line). (For interpretation of the references to colour in this figure legend, the reader is referred to the web version of this article).

D_2O (6.33×10^{-6} Å^{-2}) resulted in a contrast of 4.58×10^{-6} Å^{-2} which lead to the scattering spectra from two component system. The volume of the sulfonic groups and their contribution to the scattering are considered to be negligible. Simulations result in an average radius of 13.45 ± 0.2 Å and polydispersity of 0.43 for a sphere packing volume of 19.8% with a low q upturn with a power law decay of −2.98. Although *ex-situ* water uptake measurement of SPTES-50 at 25 °C shows 50 vol% water, it appears that not all of the water is contained in the spherical domains. It is likely that the water molecules are partially contained in the ionic aggregates and partially formed larger water pockets in the membrane. The low q upturn with a power law decay of −2.98 is attributed to the presence of interparticle interactions.

4.3.2. Hydrated SPTES-50 membrane at 55 °C

The scattering intensity increased when the temperature increased to 55 °C. The model of polydisperse spheres with liquid-like (Percus–Yevick) ordering was used to describe the q scattering spectra in the range of $0.002 < q < 0.3$ 1/Å. Optimization of the model parameters resulted in an average sphere radius of 26.4 ± 0.1 Å with a polydispersity of 0.35, hard sphere packing volume of 28.2%, and a low q power law decay of −1.1, $q\,(1/Å) < 0.006$ (see Fig. 7). Spherical ionic aggregates expand from 13.45 ± 0.05 Å to 26.4 ± 0.1 Å due to the absorption of water molecules when the temperature increased from 25 °C to 55 °C. The total *ex-situ* measured volume percent of water of the SPTES-50 increased from 50 to 78% when measured independently. The intermediate scattering power law slope decreased from −2.98 to −1.1 which is an indication of morphology changes upon increasing temperature and absorption of more water molecules. The suggested morphology is formation of interconnected cylindrical network formed due to the high volume fraction of water. The high q scattering spectra (see Fig. 7) exhibits a power law decay of −4 indicating the presence of sharp interface which can be attributed to the interface between hydrophobic and hydrophilic region. This high q Porod scattering behavior has been reported for Nafion too [22,23].

Limiting values of the Porod plot (Iq^4 *versus* q) of hydrated SPTES-50 membrane at 25 and 55 °C were 9.35×10^{-12} and 4.31×10^{-12} 1/Å^5, respectively (see Fig. 8 and Table 3). The interfacial area per unit of scattering volume of the hydrated SPTES-50 decreased from 0.072 Å^2/Å^3 at 25 °C to 0.0327 Å^2/Å^3 at 55 °C (see Table 3). This is consistent with increase of the size of spherical

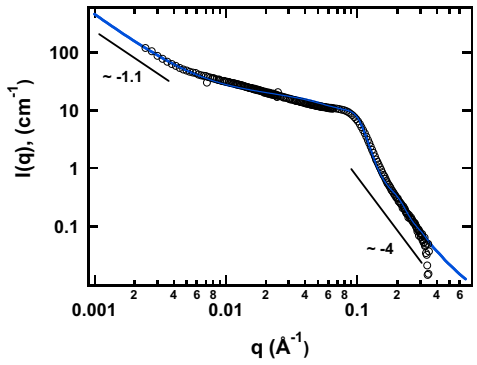

Fig. 7. SANS pattern of the hydrated SPTES-50 membrane at 55 °C (○) and fitted model of polydiperse hard sphere with Percus–Yevick liquid-like ordering assuming $R_{HS} = R$ (solid blue line). The model corresponds to membranes containing aqueous nanodomains with a radius of R = 26.4 ± 0.1 Å and a polydispersity of 0.35. (For interpretation of the references to colour in this figure legend, the reader is referred to the web version of this article).

nanodomains with increasing temperature as the sphere packing volume is more significant (28.2% *versus* 19.8%). The interfacial area per unit of scattering volume for a sphere is inversely proportion to the radius ($\sum = 3\phi_w/R$) for spherical domains. The spherical nanodomains radius of 25.9 ± 1 Å was calculated for hydrated SPTES-50 membrane at 55 °C where the Porod behavior is more prominent. This value was in excellent agreement with the average sphere radius calculated from the simulations. The spherical aggregate radius calculated for hydrated SPTES-50 membrane at 25 °C from Porod analysis was 8.3 ± 0.2 Å which was smaller than the simulation prediction (13.45 Å). This could be attributed to the more diffuse interface between water and the polymer and less pronounced Porod behavior. The limiting value for the Porod plot is more defined as temperature increased to 55 °C and 77 °C which indicates a more distinct the water–polymer interface at higher temperature. This is due to the higher diffusion rate of water molecules at higher temperature, increased vibrational motion of the polymer backbone and the sulfonic acid groups.

The scattering invariants were calculated from the area under the curve of the Iq^2 *versus* q as 8.82×10^{-11} and 7.0×10^{-11} Å^{-4} for hydrated SPTES-50 membrane at 25 °C and 55 °C (see Table 3). The water volume fraction can be calculated from the scattering invariant according to equation (12). The resulting values (58% and 74% for hydrated SPTES-50 membrane at 25 °C and 55 °C) for the calculated water volume fractions from the scattering invariants are in close agreement with the experimental water volume fractions (50% and 78% for hydrated SPTES-50 membrane at 25 °C and 55 °C).

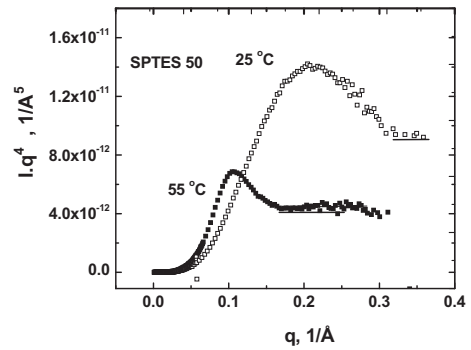

Fig. 8. Porod plot of the SANS data from hydrated SPTES-50 membrane at 25 °C (□) and 55 °C (■). The limiting value is more defined when temperature increased to 55 °C.

Table 3
Characteristics of nanodomain described by polydispersed hard sphere model with P.Y. liquid-like ordering with low q power law decay.

	Polydisperse hard sphere with P.Y. local ordering, and low q power law decay	
	Hydrated SPTES-50 membrane at 25 °C	Hydrated SPTES-50 membrane at 55 °C
Radius, Å	13.45 ± 0.05	26.4 ± 0.1
Polydispersity	0.43	0.35
Sphere volume packing	0.198	0.28
Porod limiting value[a] $1/Å^5$	9.4×10^{-12}	4.3×10^{-12}
Surface to volume ratio ($\sum$, $Å^2/Å^3$)	0.072	0.033
Radius (R, Å) (Calculated)	8.3 ± 0.2	25.9 ± 1
Scattering invariant[b]	8.82×10^{-11}	7.0×10^{-11}
Water volume fraction (ϕ_w, %) (Calculated from invariant)	58	74
Water volume fraction (ϕ_w, %) (Experimentally measured)	50	78

[a] Defined as the limit of Iq^4 for infinite q, see equation (11).
[b] See equation (12).

Hydrated SPTES-50 membrane has a segregated nanostructure consisting of hydrophilic and hydrophobic domains. The semi-rigid structure of SPTES-50 with sulfonic acid groups in the polymer backbone results in less separation of these domains compared to Nafion-117. The proton transport mechanism is strongly correlated with the nanostructure of ionic aggregates resulting from the morphology of the ionomer. This study suggests that the morphology of hydrated SPTES-50 membrane can be described by a model assuming spherical ionic domains containing water molecule in the semi-rigid polymer matrix of SPTES-50 with liquid-like ordering. The size of the ionic domains containing water molecules increased with increasing temperature to 55 °C, however, it did not show further increase with increasing temperature to 77 °C where the water volume fraction increased to 81%. This may also suggest that the ionic aggregate size has reached to the maximum possible capacity of holding water molecules and the excess amount of the adsorbed water is contained in larger scale domains. The low q upturn both at 25 °C, 55 °C, and 77 °C suggests the presence of larger scale features. The presence of a power law decay of −1.1 suggests a change in morphology at the larger scale, presumably a fractal morphology or an interconnected cylindrical network morphology at 55 °C and 77 °C. HR-TEM showed the presence of spherical aggregates of exchanged cations which were formed within ionic clusters of sulfonic acid groups. Formation of inverted micelle of hydrophilic nanodomains within the hydrophobic SPTES polymer membrane is suggested both by SANS scattering spectra as well as TEM studies. The maximum observed in the scattering spectra of the hydrated SPTES-50 membrane at 55 °C and 77 °C can be due to the excluded volume effect arising from short range liquid-like ordering or due to a change in structural factor arising from closer packing of the nanodomains. This could result in facilitated proton charge carriers transport from one nanocluster to the next one in a closer spatial distance. The number density of ionic clusters remained approximately constant ($\sim 1.18 \times 10^{17}$ cm^3), indicating that the additional water adsorbed by the polymer at the elevated temperature did not result in substantial coalescence of the clusters. This in turn suggests that the excess water is contained in a larger scale features, e.g. water pockets in the pores of the membrane at 25 °C and water networks at 55 °C and 77 °C.

5. Conclusions

SPTES-50 can be solvent cast into a tough film with high proton conductivity (135 mS/cm at 85 °C, 85% RH) which makes it a promising copolymer film for hydrogen fuel cell applications. The proton conductivity of the SPTES-50 membrane highly depends on the temperature and the water content (RH). SANS examinations in dry and swollen states (25 °C, 55 °C and 77 °C) over a wide q range illustrated the presence of a two-phase morphology consisting of ionic clusters with water molecules and hydronium ions and hydrophobic polymer. The scattering data of the hydrated membranes were evaluated using polydisperse hard sphere model with Percus–Yevick liquid-like ordering and a low q power law decay to obtain structural information regarding the average domain sizes, polydispersity and correlation between particles and particle packing volume. This model proved to be a good approximation to describe the aggregate shape, size and polydispersity of hydrated SPTES-50 membrane both at 25 °C and 55 °C. Excess adsorbed water remains in the larger water domains. The low q power law decay changed from −3 to −1.1 upon increasing temperature to 55 °C and 77 °C which indicated a change in the large scale morphology. The presence of a power law decay of −4 at large angles indicated the presence of a segregated structure with a sharp interface between the copolymer and water which was more prominent at 55 °C and 77 °C. The size of spherical aggregates in the water domain increased elevated temperature and provided higher proton conductivity. The presence of spherical ionic aggregates was suggested by HR-TEM of a silver exchanged SPTES-50 membrane at 25 °C.

Acknowledgments

The authors would like to thank the Air Force Office of Scientific Research and Materials and Manufacturing Directorate, Nanostructured and Biological Materials Branch for supporting this research. The National Institute of Standards and Technology is thanked for funding to conduct neutron scattering experiments under agreement DMR-9986442. The authors also would like to thank helpful discussions with Derek Hu (from NIST), Dr. Richard A. Vaia and Michael F. Durstock (from AFRL/RXBN).

References

[1] Dimitrova P, Friedrich KA, Stimming U, Vogt B. Solid State Ionics 2002;150:115–22.
[2] Yang C, Srinivasa S, Benziger J, Bocarsly AB. J Power Sources 2001;103:1–9.
[3] Kreuer KD. J Membr Sci 2001;185(1):29–39.
[4] Rollet AL, Diat O, Gebel G. J Phys Chem B 2004;108(3):1130–6.
[5] Essafi W, Gebel G, Mercier R. Macromolecules 2004;37(4):1431–40.
[6] Fu Yz. J Power Sources 2006;157(1):222–5.
[7] Benoit L, Patric J. J Polym Sci Part A Polym Chem 2007;45(2):269–83.
[8] Bai Z, Price GE, Yoonessi M, Juhl SB, Durstock MF, Dang TD. J Membr Sci 2007;305:69–76.
[9] Yoonessi M, Bai Z, Dang TD. J Polym Sci Part B Polym Phys 2007;45:2813–22.
[10] Bai Z, Dang TD. Macromol Rapid Commun 2006;27:1271–7.
[11] Bai Z, Durstock MF, Dang TD. J Membr Sci 2006;281:508–16.
[12] Eisenberg A, Hird B, Moore RB. Macromolecules 1990;23:4098–107.
[13] Rubatat L, Gebel G, Diat O. Macromolecules 2004;37(20):7772–83.
[14] Gottesfeld S, Zawodzinski TA. In: Alkire RC, Geridches H, Kdb DM, Tobias CW, editors. Advances in electrochemical science and engineering, vol. 5. New York: Wiley-VCH; 1997. p. 195.

[15] Serpico JM, Ehrenberg SG, Fontanella JJ, Jiao X, Perahia D, McGrady KA, et al. Macromolecules 2002;35(15):5916–21.
[16] Szajdzinska-Pietek E, Schlick SJ. J Mol Liq 2005;117(1–3):153–64.
[17] Hsu WY, Gierke TD. Macromolecules 1982;15(1):101–5.
[18] Fujimura M, Hashimoto T, Kawai H. Macromolecules 1982;15:136–44.
[19] Haubold HG, Vad T, Jungbluth H, Hiller P. Electrochim Acta 2001;46:1559–63.
[20] Gebel G. Polymer 2000;41:5829–38.
[21] Dreyfus B. Macromolecules 1985;18(2):284–92.
[22] Diat O, Gebel G. Nat Mater 2008;7:13–4.
[23] Schmidt-Rohr K, Chen Q. Nat Mater 2007;7:75–83.
[24] Porod G. In: Glatter O, Kratky O, editors. Small-angle X-ray scattering. London: Academic Press; 1982. p. 17.
[25] Higgins JS, Benoit HC. Polymers and neutron scattering. Oxford: Clarendon Press; 1994. p. 134.
[26] Griffith ML, Triolo R, Compere AL. Phys Rev A 1987;35:2200–6.
[27] Kinning DJ, Thomas EL. Macromolecules 1984;17:1712–8.
[28] Yeo RS. J Electrochem Soc 1983;130(3):533–8.
[29] Ma C, Zhang L, Mukerjee S, Ofer D, Nair B. J Membr Sci 2003;219:123–36.